the preparation of acetyl-Phe-Leu-2-thiohydantoin, and preliminary studies on a stepwise solution phase carboxyl-terminal degradation (4 pages). Ordering information is given on any current masthead page.

References

Ambler, R. P. (1967a) *Methods Enzymol. 11*, 155.
Ambler, R. P. (1967b) *Methods Enzymol. 11*, 436.
Cromwell, L. D., & Stark, G. R. (1969) *Biochemistry 8*, 4735.
Darbre, A. (1977) *Methods Enzymol. 47*, 357.
Darbre, A., & Rangarajan, M. (1975) in *Solid Phase Methods in Protein Sequence Analysis* (Laursen, R. A., Ed.) p 131, Pierce Chemical Co., Rockford, IL.
Dwulet, F. E. (1976) Ph.D. Thesis, Indiana University.
Dwulet, F. E., & Gurd, F. R. N. (1977) *Anal. Biochem. 82*, 385.
Dwulet, F. E., & Gurd, F. R. N. (1979) *Int. J. Pept. Protein Res. 13*, 122.
Dwulet, F. E., Bogardt, R. A., Jones, B. N., Lehman, L. D., & Gurd, F. R. N. (1975) *Biochemistry 14*, 5336.
Dwulet, F. E., Jones, B. N., Lehman, L. D., & Gurd, F. R. N. (1977) *Biochemistry 16*, 873.
Edman, P. (1950) *Acta Chem. Scand. 4*, 277.
Edmundson, A. B. (1965) *Nature (London) 205*, 883.
Hapner, K. D., Bradshaw, R. A., Hartzell, C. R., & Gurd, F. R. N. (1968) *J. Biol. Chem. 243*, 683.
Kubo, H., Nakarjima, T., & Tamura, Z. (1971) *Chem. Pharm. Bull. 19*, 210.
Laursen, R. A. (1966) *J. Am. Chem. Soc. 88*, 5344.
Laursen, R. A. (1971) *Eur. J. Biochem. 20*, 89.
Laursen, R. A., & Machleidt, W. (1980) *Methods Biochem. Anal. 26*, 201.
March, K. L., Maskalick, D. G., England, R. D., Friend, S. H., & Gurd, F. R. N. (1982) *Biochemistry* (in press).
Rangarajan, M., & Darbre, A. (1975) *Biochem. J. 147*, 435.
Rangarajan, M., & Darbre, A. (1976) *Biochem. J. 157*, 307.
Rangarajan, M., Ardrey, R. E., & Darbre, A. (1973) *J. Chromatogr. 87*, 499.
Robinson, P. J., Dunnill, P., & Lilly, M. D. (1971) *Biochim. Biophys. Acta 242*, 659.
Schlack, P., & Kumpf, W. (1926) *Hoppe-Seyler's Z. Physiol. Chem. 154*, 126.
Schlesinger, D. H., Weiss, J., & Audhya, T. K. (1979) *Anal. Biochem. 95*, 494.
Schmitt, H. W., & Walker, J. E. (1977) *FEBS Lett. 81*, 403.
Scoffone, E., & Turco, A. (1956) *Ric. Sci. 26*, 865.
Staab, H. A. (1962) *Angew. Chem., Int. Ed. Engl. 1*, 351.
Stark, G. R. (1968) *Biochemistry 7*, 1796.
Stark, G. R. (1972) *Methods Enzymol. 25*, 369.
Stewart, J. M., & Young, J. D. (1969) *Solid Phase Peptide Synthesis*, Chapter 2, W. H. Freeman, San Francisco, CA.
Stokes, H. N., & Cain, J. R. (1907) *J. Am. Chem. Soc. 29*, 443.
Tarr, G. E. (1977) *Methods Enzymol. 47*, 335.
Venter, J. C., & Dixon, J. E. (1974) *Methods Enzymol. 38*, 180.
Walsh, K. A., Ericsson, L. H., Parmelee, D. C., & Titani, K. (1981) *Annu. Rev. Biochem. 50*, 261.
Williams, M. J., & Kassell, B. (1975) *FEBS Lett. 54*, 353.
Yamashita, S. (1971) *Biochim. Biophys. Acta 229*, 301.
Yamashita, S., & Ishikawa, N. (1972) in *Chemistry and Biology of Peptides: Proceedings of the Third American Peptide Symposium* (Meienhofer, J., Ed.) p 701, Ann Arbor Science Publishers, Ann Arbor, MI.

Kinetic Mechanism of the Reaction Catalyzed by Dihydrofolate Reductase from *Escherichia coli*†

Stuart R. Stone and John F. Morrison*

ABSTRACT: The kinetic mechanism of the reaction catalyzed by dihydrofolate reductase from *Escherichia coli* has been investigated by using progress curve, initial velocity, product inhibition, and dead-end inhibition studies as well as isotope effects. The results indicate that the reaction conforms to a random mechanism involving two dead-end complexes, viz., enzyme–DHF–THF and enzyme–NADP–DHF. At higher concentrations, DHF causes substrate inhibition by combining at the NADPH binding site on the enzyme. The steady-state velocity data can be analyzed adequately on the basis that rapid-equilibrium conditions apply. However, this can be only an approximate description of the reaction since the isotope effects observed with NADPD demonstrate clearly that catalysis cannot be rate limiting at pH 7.4. The choice of conditions for analysis of progress-curve data is discussed in the Appendix.

Dihydrofolate reductase (5,6,7,8-tetrahydrofolate:NADP$^+$ oxidoreductase, EC 1.5.1.3) catalyzes the NADPH-dependent reduction of 7,8-dihydrofolate (DHF)[1] to 5,6,7,8-tetrahydrofolate (THF). THF is an essential cofactor in a number of one-carbon transfer reactions including the biosynthesis of thymidylate. Thus, inhibition of dihydrofolate reductase can lead to a deficiency of thymidylate and to the disruption of DNA biosynthesis. Inhibitors of the enzyme have found clinical applications in the treatment of neoplastic and microbial diseases (Blakley, 1969). Because of its pharmacological importance, dihydrofolate reductase has been studied extensively (Gready, 1981), but despite the many detailed studies on the enzyme, its kinetic mechanism has not been established. It has been proposed that the reaction catalyzed

† From the Department of Biochemistry, John Curtin School of Medical Research, Australian National University, Canberra City A.C.T. 2601, Australia. *Received January 5, 1982.*

[1] Abbreviations: DHF, 7,8-dihydrofolate; THF, 5,6,7,8-tetrahydrofolate; Tris, tris(hydroxymethyl)aminomethane; Mes, 4-morpholineethanesulfonic acid.

0006-2960/82/0421-3757$01.25/0

by the enzyme from *Streptococcus faecium* conforms to a steady-state ordered mechanism (Blakley et al., 1971) whereas that from *Escherichia coli* catalyzes a rapid-equilibrium random mechanism (Burchall & Chan, 1969; McCullough et al., 1971).

Kinetic studies on the dihydrofolate reductase reaction have been hampered by the low values for the Michaelis constants which are micromolar or lower for both substrates. It appeared that there may well be merit in applying to the dihydrofolate reductase reaction the protocols developed by Duggleby & Morrison (1977–1979) for the elucidation of the kinetic mechanism of enzyme-catalyzed reactions by analysis of progress-curve data. The results of this approach have been compared with those obtained by use of initial, steady-state velocity studies. The data indicate that the reaction conforms to a random mechanism which involves the formation of two dead-end complexes and that, at higher concentrations, DHF can react at the binding site for NADPH.

Experimental Procedures

Materials. DHF was obtained by chemical reduction of folic acid as described by Blakley (1960). THF, prepared by enzymic reduction of DHF, was purified according to the method of Zakrzewski & Sansone (1971) and contained 2–3% DHF. NADPD was prepared from NADP and ethanol-*d* by using alcohol dehydrogenase from *Leuconostoc mesenteroides*. The product was purified by the method of Viola et al. (1979). Enzymes were obtained from Boehringer Mannheim while all other chemicals were of the highest purity available commercially. The concentrations of THF, DHF, and 2′-AMP were determined spectrophotometrically by using extinction coefficients of 28 mM^{-1} cm^{-1} at 297 nm (Zakrzewski & Sansone, 1971), 28 mM^{-1} cm^{-1} at 282 nm, and 15.3 mM^{-1} cm^{-1} at 260 nm (Dawson et al., 1969), respectively. NADP was estimated enzymically by using glucose-6-phosphate dehydrogenase. Dihydrofolate reductase was used to estimate the concentrations of NADPH and DHF; the millimolar absorbance change of the reaction was taken to be 11.8 cm^{-1} (see below). Dihydrofolate reductase was purified from a strain of *Escherichia coli* which was produced by in vitro mutagenesis of the DNA of the plasmid pJFM 8 (Rood et al., 1980; Rood & Williams, 1981). The enzyme was purified essentially as described by Williams et al. (1979).

Enzyme Assays. Dihydrofolate reductase was assayed by measuring, with a Cary 118 spectrophotometer, the rate of enzyme-dependent decrease in the absorbance at 340 nm. For determination of the molar absorbance change, reaction mixtures contained 100 μM NADPH and about 6 μM dihydrofolate. The reaction was started by the addition of 4.6 nM dihydrofolate reductase and allowed to proceed to completion. The amount of NADP formed was measured by using glucose-6-phosphate dehydrogenase and taking into account the amount of NADP present initially as a contaminant of the NADPH. The results of nine replicate determinations indicated that the millimolar absorbance change at 340 nm of the dihydrofolate reductase reaction was 11.8 ± 0.5 cm^{-1}. This value, which has been used throughout the present study, compares well with the value of 12.3 cm^{-1} obtained by Hillcoat et al. (1967).

Initial rate assays were performed in cuvettes of 1.0-cm light path which contained 0.05 M Tris, 0.025 M acetate, 0.025 M Mes buffer (pH 7.4), 0.1 M NaCl, and 10 mM dithiothreitol (buffer A), as well as substrates, in a final volume of 1.0 mL. The assays were started by the addition of dihydrofolate reductase (0.46–13.8 nM). In the absence of the enzyme the rate of change of absorbance was negligible. At low substrate concentrations, it was necessary to note the time of enzyme addition and to use ship curves[2] for determination of initial rates. Enzyme concentration was determined as described by Williams et al. (1979). When THF was used in product inhibition studies, allowance was made for its contamination by DHF.

For progress-curve experiments, the two-substrate reaction of dihydrofolate reductase was reduced to a one-substrate irreversible reaction by one of two means: (1) one of the substrates was set at a concentration such that it would remain essentially constant for the entire progress curve, or (2) NADP was recycled to NADPH by using glucose-6-phosphate dehydrogenase (cf. Duggleby & Morrison, 1977). For the first method, the reaction conditions were the same as those used for initial rate experiments, and the reaction was started by the addition of 1.4–23 nM dihydrofolate reductase. When NADP was recycled, the assay contained buffer A, 10 mM glucose 6-phosphate, glucose-6-phosphate dehydrogenase (6 units), and substrates in a final volume of 1.0 mL; the reaction was started by the addition of 9.2–138 nM dihydrofolate reductase. The method of Selwyn (1965) was used to establish the absence of time-dependent inactivation of dihydrofolate reductase under progress-curve conditions. This method also indicated that there was no lag in the formation of tetrahydrofolate when NADP was recycled to NADPH.

Equilibrium Dissociation Constants. Equilibrium dissociation constants for enzyme–ligand complexes were determined by fluorescence titration at 30 °C by using a Perkin-Elmer 3000 spectrofluorometer. Excitation and emission wavelengths were 290 and 340 nm, respectively. Titrations were carried out by serial additions of aliquots (1–4 μL) of ligand to a 1.0-cm^2 quartz cuvette that contained a solution of dihydrofolate reductase in buffer A. A standard tryptophan solution was titrated, and the results were used to correct for light absorption by added ligands. Equilibrium fluorescence readings were recorded 2 min after the addition of the ligand, and the dissociation constants were estimated by nonlinear regression as described below. None of the ligands contributed to the fluorescence.

Data Analysis. Initial rate data were analyzed by using weighted nonlinear regression. The computer program, which was a modified version (Duggleby & Morrison, 1979) of one written by C. W. Jackson and J. P. Chandler, was obtained in the STEPT package (QCPE 307) from the Quantum Chemistry Program Exchange at Indiana University. The weighting used in the fitting assumed standard errors in the initial velocities proportional to the velocities. The significance of the extra parameter in noncompetitive inhibition analyses was tested by using an *F* test (Pollard, 1977).

The progress curve for any irreversible reaction in which only one substrate is depleted can be described by the general equation (Duggleby & Morrison, 1979)

$$R_1 t = Z + \frac{R_2 Z^2}{2} - R_3 \ln\left(1 - \frac{Z}{A_0}\right) \qquad (1)$$

where Z is the amount of product formed at time t, A_0 is the initial concentration of the substrate being depleted, and R_1, R_2, and R_3 are parameters dependent on the kinetic constants of the reaction together with the initial concentrations of products and substrates. A progress-curve experiment consisted of a number of progress curves obtained at different

[2] Ship curves are special designs of French curves which are used in connection with nautical design. They are constructed of clear plastic and allow determination of tangents to the initial part of a curve.

initial concentrations of the substrates in the absence or presence of products. From each progress curve, 15–20 data points were taken over the range of 10–98% substrate utilization. These data were fitted to eq 1 by using the PROCURA computer program of Duggleby & Morrison (1977). This analysis yielded values for R_1, R_2, and R_3 together with their standard errors; the values were used to compress the data from each curve into three theoretical points as recommended by Duggleby & Morrison (1978). The compressed data points from all the progress curves in an experiment were then fitted to a number of equations and that which best fitted the data was chosen on the basis of the variance values and when necessary after the application of an F test (Pollard, 1977). Compressed data sets were obtained by taking three theoretical points which corresponded to the times for 10% and either 95% (condition 1) or 98% (condition 2) substrate utilization as well as a point midway between these two times.

The fluorescence of dihydrofolate reductase in the presence of a ligand can be represented by

$$F = [F_0(E_t - EL) + F_\infty(EL)]/(E_t) \quad (2)$$

where F, F_0, and F_∞ are the observed fluorescence, the fluorescence of the free enzyme, and the fluorescence of the enzyme–ligand complex, respectively; (L_t), (EL), (E_t), and $(E_t - EL)$ denote the concentrations of total ligand, the enzyme–ligand complex, the total enzyme, and free enzyme, respectively. The dissociation constant (K_d) for the enzyme–ligand complex is given by

$$K_d = (E_t - EL)(L_t - EL)/(EL) \quad (3)$$

Estimates for F_0, F_∞, and K_d were obtained by fitting fluorescence titration data to eq 2 and 3. The program used for this nonlinear regression was developed from the STEPT package.

Results

Progress-Curve Experiments with Recycling of NADP. Progess-curve experiments were performed by recycling NADP to NADPH at five different concentrations of NADPH that ranged from 0.3 to 3.0 μM. Four initial concentrations of THF from 0 to 40 μM were used at each NADPH concentration; the initial concentrations of DHF varied from 10 to 15 μM. The data from each of these curves were compressed as described under Experimental Procedures and fitted to different integrated rate equations that describe possible mechanisms for the dihydrofolate reductase reaction. Twelve possible mechanisms were considered: two steady-state ordered mechanisms, two Theorell–Chance mechanisms, four rapid-equilibrium random mechanisms, and four rapid-equilibrium ordered mechanisms (Table I). The steady-state ordered mechanism with DHF adding first (mechanism 2), both Theorell–Chance mechanisms, and the rapid-equilibrium random mechanism with an enzyme–NADPH–THF dead-end complex yielded the same equation. Thus, the data were fitted to nine equations. The values for the residual sum of squares obtained by fitting to each equation the progress-curve data from experiments under two different conditions of data compression are given in Table I.

When condition 1 was applied to compress data from the two experiments, the equation yielding the lowest residual sum of squares represented a rapid-equilibrium random mechanism in which an enzyme–DHF–THF dead-end complex forms (mechanism 4). A slightly larger value for the sum of squares was obtained with a rapid-equilibrium ordered mechanism in which DHF was the first substrate to add to the enzyme and in which an enzyme–DHF–THF dead-end complex forms (mechanism 9). All except one of the remaining fits contained values for one or more of the kinetic parameters which were negative or greater than 1 M. The equation for mechanism 4 has one more parameter than that for mechanism 9. When the significance of this parameter was tested by means of an F test, the reduction in the sum of squares caused by the inclusion of this term was found to be nonsignificant. Therefore, for these sets of compressed data, the rapid-equilibrium ordered mechanism (mechanism 9) must be preferred.

When condition 2 was applied to compress the data, the best fit was obtained with a rapid-equilibrium random mechanism in which there is formed both an enzyme–DHF–THF and an enzyme–NADPH–THF dead-end complex (mechanism 5). The equation for mechanism 4 yields a slightly larger sum of squares in one of the two experiments. The integrated rate equation for mechanism 5 contains an extra parameter which is associated with the enzyme–NADPH–THF complex. The reduction in the sum of squares caused by this parameter was found to be significant in one experiment and nonsignificant in the other. Thus, the most appropriate mechanism as judged by an F test on the residual sum of squares varied with both the experiment and the conditions of data compression. Although it is not possible to choose unequivocally between the possible mechanisms, the rapid-equilibrium random mechanism in which a single ternary dead-end complex forms (mechanism 4) must be preferred because the equation describing this mechanism gave a low residual sum of squares under both conditions of data compression and in both experiments. The values of the parameters obtained by using the appropriate equation for mechanism 4 are given in Table

Table I: Residual Sum of Squares Obtained by Fitting Progress-Curve Data to Various Models[a]

	residual sums of squares (μM²) data compression			
	condition 1		condition 2	
mechanism	expt 1	expt 2	expt 1	expt 2
(1) steady state ordered, NADPH first	0.85[c]	0.72[c]	0.49[c]	0.49[c]
(2) steady state ordered, DHF first[b]	0.77[c]	0.80	1.94[c]	0.59
(3) rapid equilibrium random	0.77[c]	0.90[c]	0.51[c]	0.69[c]
(4) rapid equilibrium random with E-DHF-THF	0.43	0.69	0.26	0.54
(5) rapid equilibrium random with E-DHF-THF and E-NADPH-THF	0.43[c]	1.02	0.26	0.44
(6) rapid equilibrium ordered, NADPH first	1620[c]	23[c]	2220[c]	1480[c]
(7) rapid equilibrium ordered, DHF first	0.77[c]	0.90[c]	0.51[c]	0.69[c]
(8) rapid equilibrium ordered, NADPH first with E-NADPH-THF	3.8[c]	3.0[c]	2.8	2.4
(9) rapid equilibrium ordered, DHF first with E-DHF-THF	0.44	0.70	0.84	1.0

[a] Progress-curve experiments were performed by recycling NADP to NADPH at various levels of NADPH and THF. Data from each curve were fitted to eq 1, compressed according to either condition 1 or condition 2, and then fitted to the integrated rate equation for each mechanism. [b] The integrated rate equation for this mechanism is identical with those for the two Theorell–Chance mechanisms and for a rapid-equilibrium random mechanism with a dead-end enzyme–NADPH–THF complex. [c] These fits yielded one or more parameter values that were either negative or greater than 1 M.

Table II: Kinetic Parameters Associated with the Dihydrofolate Reductase Reaction[a]

parameter	initial rate: NADP recycled	initial rate: no recycling of NADP	weighted[c] mean	progress curve: NADP recycled, condition 1[d]	progress curve: NADP recycled, condition 2[d]	progress curve: one substrate[b] saturating
V_1 (min^{-1})	1080 ± 40	950 ± 30	990 ± 20	880 ± 134	830 ± 140	
K_{ia} (μM)[e]	4.2 ± 0.7	3.5 ± 0.6	3.8 ± 0.5	2.3 ± 2.0	1.9 ± 1.5	
K_a (μM)	2.4 ± 0.2	2.7 ± 0.2	2.5 ± 0.1	1.9 ± 0.4	1.9 ± 0.5	1.4 ± 0.2
K_{ib} (μM)	1.0 ± 0.2	0.7 ± 0.1	0.76 ± 0.09	1.9 ± 2.3	2.2 ± 2.2	0.60 ± 0.17
K_b (μM)	0.56 ± 0.08	0.43 ± 0.06	0.47 ± 0.05	1.5 ± 1.2	1.6 ± 1.3	

[a] Details of the experimental procedures are given in the text, and kinetic parameters are as defined in Scheme I. [b] Either NADPH or DHF was present at a concentration of 100 μM. [c] Weighted mean values were calculated by using data obtained from four experiments. [d] The two conditions of data compression are described in the text. [e] A and B denote NADPH and DHF, respectively, while the corresponding lower case letters are used for the kinetic constants associated with these substrates.

Table III: Inhibition Constants for Products of Dihydrofolate Reductase Reaction[a]

product inhibitor	variable substrate(s)	type of experiment	fixed concn of other substrate (μM)	type of inhibition	inhibition constant	K_i value (μM): apparent	K_i value (μM): true	reaction
THF	DHF	i.v.[b]	0.5	NC	K_{ip}	4.0 ± 0.4	3.5 ± 0.3[c]	E + THF
					K_{Ip}	7.6 ± 0.8	6.4 ± 0.7[d]	E-DHF + THF
		i.v.	100	C	K_{ip}	20 ± 1	0.7 ± 0.1[c]	
		p.c.	100	C	K_{ip}	29 ± 6	1.0 ± 0.3[c]	
	NADPH	i.v.	2.5	C	K_{is}	4.7 ± 0.8[b] (3.7 ± 0.7)[e]		
		p.c.	100	C	K_{Ip}		37 ± 5[f]	
	DHF + NADPH	p.c.	*i*		K_{ip}		4.8 ± 1.8[f]	
					K_{Ip}		22 ± 5[f]	
NADP	DHF	i.v.	0.93	NC	K_{iq}	48 ± 9	39 ± 7[g]	E + NADP
					K_{Iq}	23 ± 2	17 ± 1[h]	E-DHF + NADP
	NADPH	i.v.	1.74	C	K_{is}	13 ± 1 (20 ± 2)[e]		
		p.c.	100	C	K_{Iq}		12 ± 1[f]	

[a] Apparent values for kinetic parameters were obtained by analysis of initial rate data, including those illustrated in Figures 2 and 3. True values were determined from the apparent values by using the appropriate relationships together with the concentrations of the nonvaried substrates and the values for the required kinetic constants that are given in Table II. A, B, P, and Q denote NADPH, DHF, THF, and NADP, respectively. [b] i.v., initial velocity data; p.c., progress-curve data. [c] Calculated using $K_{ip} = {}^{app}K_{ip}/(1 + A/K_{ia})$. [d] Calculated using $K_{Ip} = {}^{app}K_{Ip}/(1 + A/K_a)$. [e] Values given in parentheses are apparent inhibition constants which were calculated for comparison with the directly observed values. The relationships used with initial velocity data obtained at fixed DHF (B) concentration were $K_{is} = (1 + K_{ib}/B)/(1/K_{Ip} + K_{ib}/K_{ip}B)$ with THF as product inhibitor and $K_{is} = (1 + K_{ib}/B)/(1/K_{Iq} + K_{ib}/K_{iq}B)$ with NADP as product inhibitor. [f] Values obtained directly from analysis of progress-curve data. [g] Calculated using $K_{iq} = {}^{app}K_{iq}/(1 + A/K_{ia})$. [h] Calculated using $K_{Iq} = {}^{app}K_{Iq}/(1 + A/K_a)$. [i] NADP recycled.

II. The values of these parameters did not vary appreciably with the different conditions of data compression, but they were not well determined as judged by the values of their standard errors.

Progress-Curve Experiments with One Substrate at a Saturating Concentration. Analysis of progress-curve data indicated that with NADPH at 100 μM and the initial concentration of DHF at 4–8 μM, THF (0–100 μM) causes competitive inhibition with respect to DHF whereas NADP does not inhibit at concentrations up to 88 μM. With DHF fixed at 100 μM and the initial concentration of NADPH at 4–5 μM, both NADP (0–88 μM) and THF (0–100 μM) cause competitive inhibition with respect to NADPH. The inhibition constants associated with THF and NADP are given in Table III.

Initial Velocity Studies. The initial velocity pattern obtained by using both NADPH and DHF as the variable substrates was of the symmetrical, intersecting type (Figure 1). Analysis of the data yielded values for the kinetic parameters that are listed in Table II. Initial velocity data were also obtained with NADP recycled to NADPH at varying concentrations of NADPH and DHF. The values of the parameters given in Table II are not significantly different from those obtained in the absence of NADP recycling. Thus the recycling does not seem to affect the dihydrofolate reductase reaction.

Product Inhibition Studies. At nonsaturating concentrations of the fixed substrate, THF acts as a linear competitive inhibitor with respect to NADPH and as a linear noncompetitive inhibitor with respect to DHF (Figure 2). Under similar conditions, NADP causes linear competitive inhibition with respect to NADPH and linear noncompetitive inhibition with respect to DHF (Figure 2). By contrast, THF gives rise to competitive inhibition with respect to DHF when the concentration of NADPH is increased to 100 μM (Figure 3). Table III lists values for the apparent and true inhibition constants obtained by analysis of the data of Figure 2.

Inhibition by Substrate Analogues. Folate and 2′-AMP were used as analogues of DHF and NADPH, respectively. At concentrations up to 187 μM, folate does not act as a substrate for dihydrofolate reductase, but it causes linear competitive inhibition with respect to DHF and linear noncompetitive inhibition with respect to NADPH (Figure 4). 2′-AMP acts as a linear competitive inhibitor with respect to NADPH and as a linear noncompetitive inhibitor with respect to DHF (Figure 4). Analysis of the data of Figure 4 yielded the apparent values for the inhibition constants that are recorded in Table IV which also records true values for the inhibition constants.

Substrate Inhibition by DHF. Substrate inhibition by DHF was observed at concentrations greater than 33 μM when the

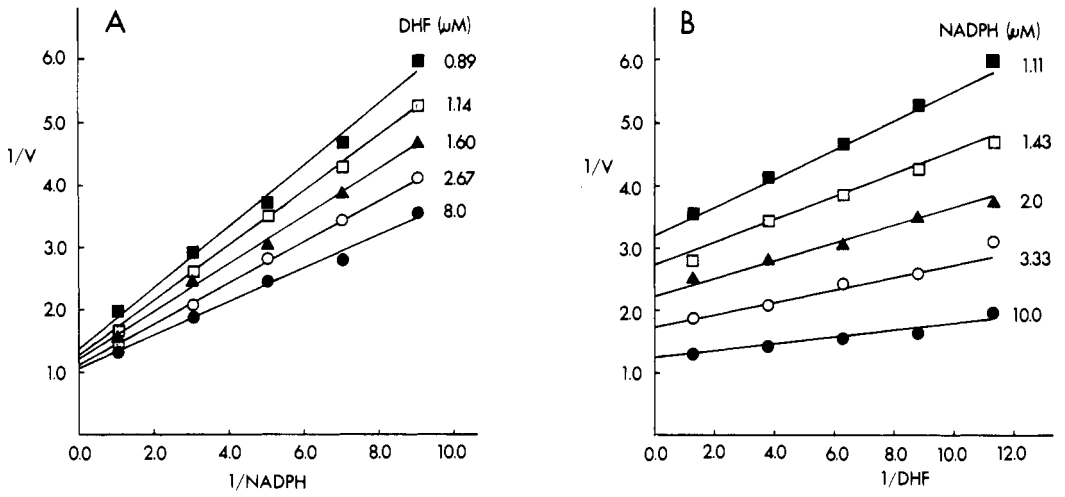

FIGURE 1: Plots of the reciprocal of initial velocity of the reaction (min × 10^3) against the reciprocal of the concentration of NADPH or DHF (M^{-1} × 10^{-5}). The concentration of enzyme was 1.8 nM.

Table IV: Kinetic Constants for Reaction of Substrate Analogues with Dihydrofolate Reductase

substrate analogue	varied substrate	fixed substrate concn (μM)	type of inhibition	inhibition constant[a] apparent (mM)	inhibition constant[a] true (mM)	reaction
2'-AMP	DHF	3.33	noncompetitive	3.1 ± 0.5	1.6 ± 0.3	E + 2'-AMP
				2.7 ± 0.5	1.2 ± 0.2	E-DHF + 2'-AMP
	NADPH	1.14	competitive	2.7 ± 0.2 (1.3 ± 0.2)[b]		
folate	NADPH	1.14	noncompetitive	0.081 ± 0.012	0.032 ± 0.005	E + folate
				0.037 ± 0.004	0.011 ± 0.001	E-NADPH + folate
	DHF	3.33	competitive	0.013 ± 0.001 (0.017 ± 0.003)		

[a] As dead-end inhibitors react in the same way as do the products of a rapid-equilibrium random mechanism, the true inhibition (dissociation) constants were calculated from apparent values by using relationships similar to those given as footnotes in Table III (cf. Smith & Morrison, 1971). [b] Figures in parentheses represent apparent inhibition constants which were calculated for comparison with the directly determined values by using relationships of similar form to those given in footnote *e* of Table II (cf. Smith & Morrison, 1971).

level of NADPH was low (1.1 μM). But in the presence of high concentrations of NADPH (100 μM), substrate inhibition by DHF was not apparent (Figure 3). NADPH did not give rise to substrate inhibition.

Equilibrium Binding Studies. The binding of DHF (0–50 μM), NADPH (0–8 μM), and NADP (0–65 μM) to the free enzyme was measured by fluorescence titration, and the dissociation constants for the reactions are given in Table V. With the range of concentrations used, there was no evidence for the binding of more than one molecule of a ligand per enzyme molecule. The equilibrium binding of THF could not be measured because of the slight contamination of THF by DHF.

Deuterium Isotope Effects. The deuterium isotope effects on the reaction catalyzed by dihydrofolate reductase were determined by conducting two initial rate experiments in which both the NADPH (or NADPD) and DHF were varied. The results showed that the isotope effect at pH 7.4 was small at 1.2 ± 0.1 for ^{D}V and not significant for $^{D}V/K_{DHF}$, $^{D}V/K_{NADPH}$, $^{D}K_{iDHF}$, and $^{D}K_{iNADPH}$.

Table V: Thermodynamic Dissociation Constants for Binding of Reactants to Dihydrofolate Reductase[a]

reactant	kinetic symbol for constant	value (μM)
NADPH	K_{ia}	0.51 ± 0.01[b]
DHF	K_{ib}	0.47 ± 0.05[c]
NADP	K_{iq}	18 ± 3[c]

[a] Values were determined by analysis of fluorescence titration data as described under Experimental Procedures. [b] Weighted mean of four determinations. [c] Weighted mean of two determinations.

Discussion

The results of progress-curve experiments in which NADP was recycled to NADPH suggest that the reaction catalyzed by dihydrofolate reductase conforms to a rapid-equilibrium random mechanism involving a single dead-end enzyme–THF–DHF complex or to the same mechanism with an additional dead-end enzyme–NADPH–THF complex (Table I). The symmetrical initial velocity pattern (Figure 1) and the dead-end inhibition pattern (Figure 4) are as predicted for a rapid-equilibrium random mechanism. The product inhibition pattern (Table III) confirms the conclusions reached from the progress-curve studies except that there was no evidence for the formation of a dead-end enzyme–NADPH–THF complex. Indeed, the competitive inhibition by THF with respect to NADPH immediately suggests a random mechanism in which such a dead-end complex does not form. Further, the product inhibition pattern indicates that a dead-end enzyme–NADP–DHF complex can be formed. Such a complex could not be observed under conditions where NADP is recycled to NADPH. Thus the results of progress-curve and steady-state velocity studies indicate that the kinetic mechanism of the dihydrofolate reductase reaction is of the rapid-equilibrium random type and involves the formation of two dead-end complexes, viz., enzyme–DHF–THF and enzyme–NADP–DHF (Scheme I).

The formation of a dead-end enzyme–DHF–THF complex is an unusual feature of the proposed mechanism. On the basis of the known three-dimensional structure of this small, monomeric enzyme (Matthews et al., 1978), it seemed likely that

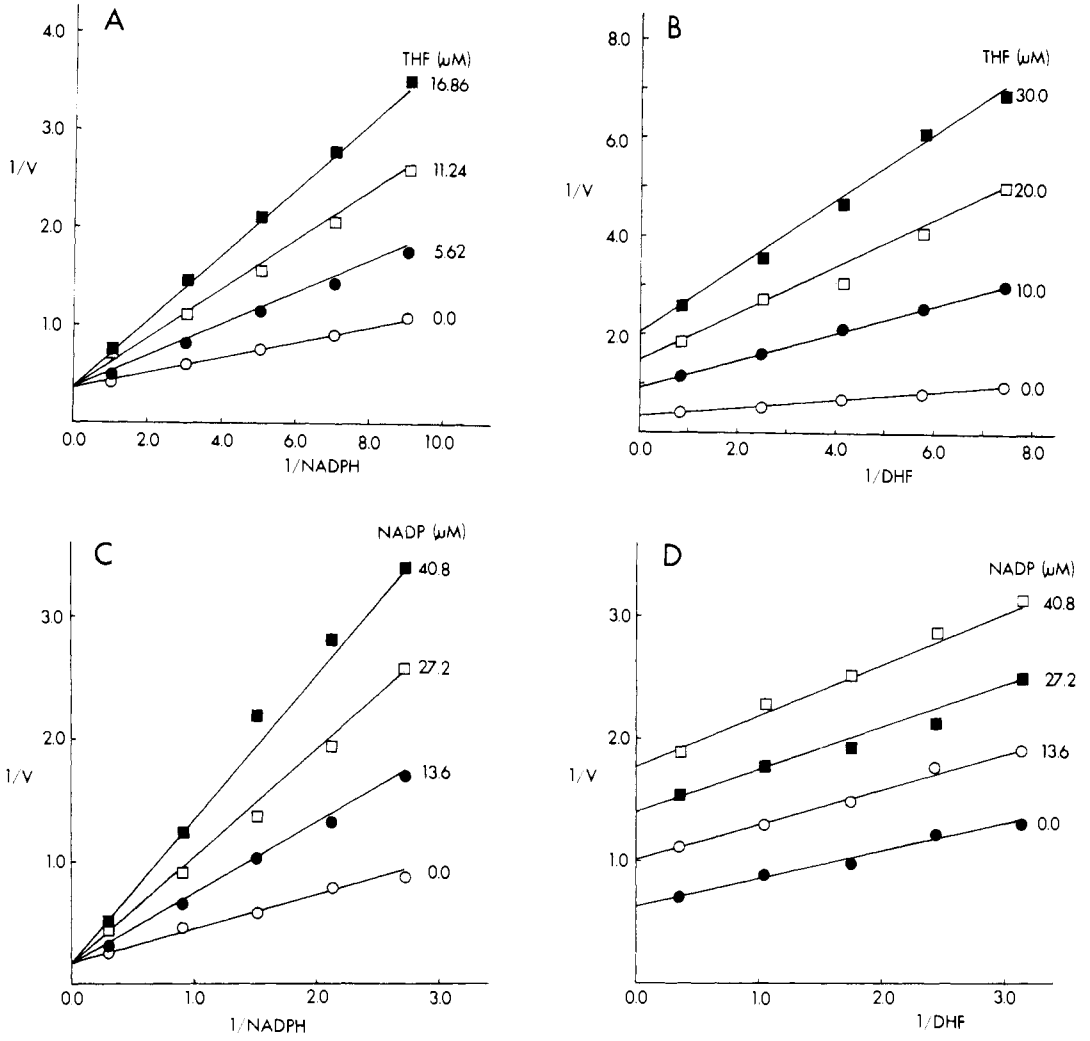

FIGURE 2: Product inhibition of the reaction by THF and NADP. Plots of the reciprocal of initial velocity of the reaction (min × 10^2) against the reciprocal of the concentration of NADPH or DHF (M^{-1} × 10^{-5}). DHF was held constant at a concentration of 2.46 μM (A) or 1.74 μM (C); the fixed concentration of NADPH was 0.5 μM (B) or 0.96 μM (D). The concentration of enzyme varied from 0.9 to 5.5 nM.

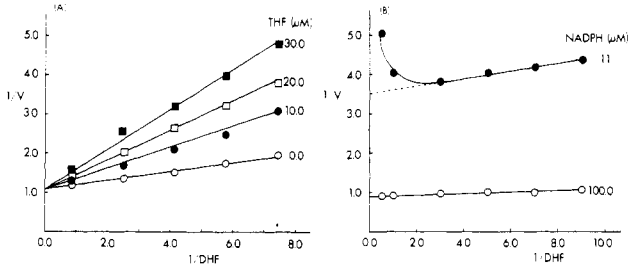

FIGURE 3: (A) Product inhibition of the reaction by THF. Plot of the reciprocal of initial velocity of the reaction (min × 10^3) against the reciprocal of DHF concentration (M^{-1} × 10^{-5}) with NADPH held constant at 100 μM. The enzyme concentration was 0.9 nM. (B) Substrate inhibition of the reaction by DHF at two concentrations of NADPH. Plot of the reciprocal of the initial velocity of the reaction (min × 10^3) against the reciprocal concentration of DHF (M^{-1} × 10^{-4}). The enzyme concentration was 0.46 nM.

Scheme I

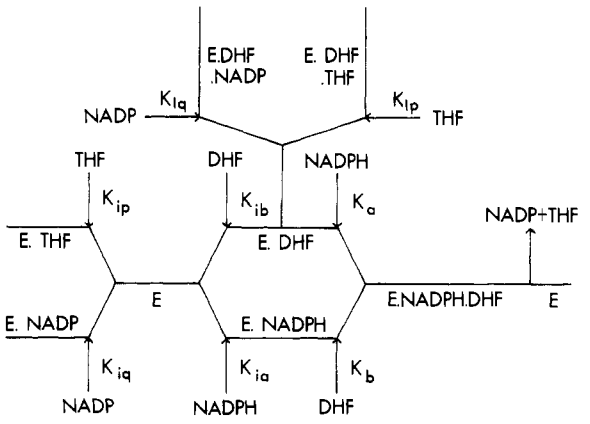

the dead-end complex forms because of the ability of THF to react at the binding site for pyridine nucleotides. This being so, it follows that the formation of the dead-end complex should be prevented at higher concentrations of NADPH, and the data (Figure 3) confirm that this is the case. Under these conditions, THF competes only with DHF for the folate binding site. DHF is also capable of interacting at the pyridine nucleotide binding site for at higher concentrations in the presence of a low level of NADPH, substrate inhibition is observed (Figure 3). These findings are of interest in view of the reports that (*p*-aminobenzoyl)glutamate causes parabolic inhibition with respect to DHF of the enzyme from *Streptococcus faecium* (Williams et al., 1980) and that two molecules of this compound are bound to the enzyme from *Lactobacillus casei* (Birdsall et al., 1977). It seems likely that both DHF and THF are bound at the pyridine nucleotide binding site through their (*p*-aminobenzoyl)glutamate moieties.

On the assumption that, for the mechanism illustrated in Scheme I, catalysis is rate limiting so that the products act

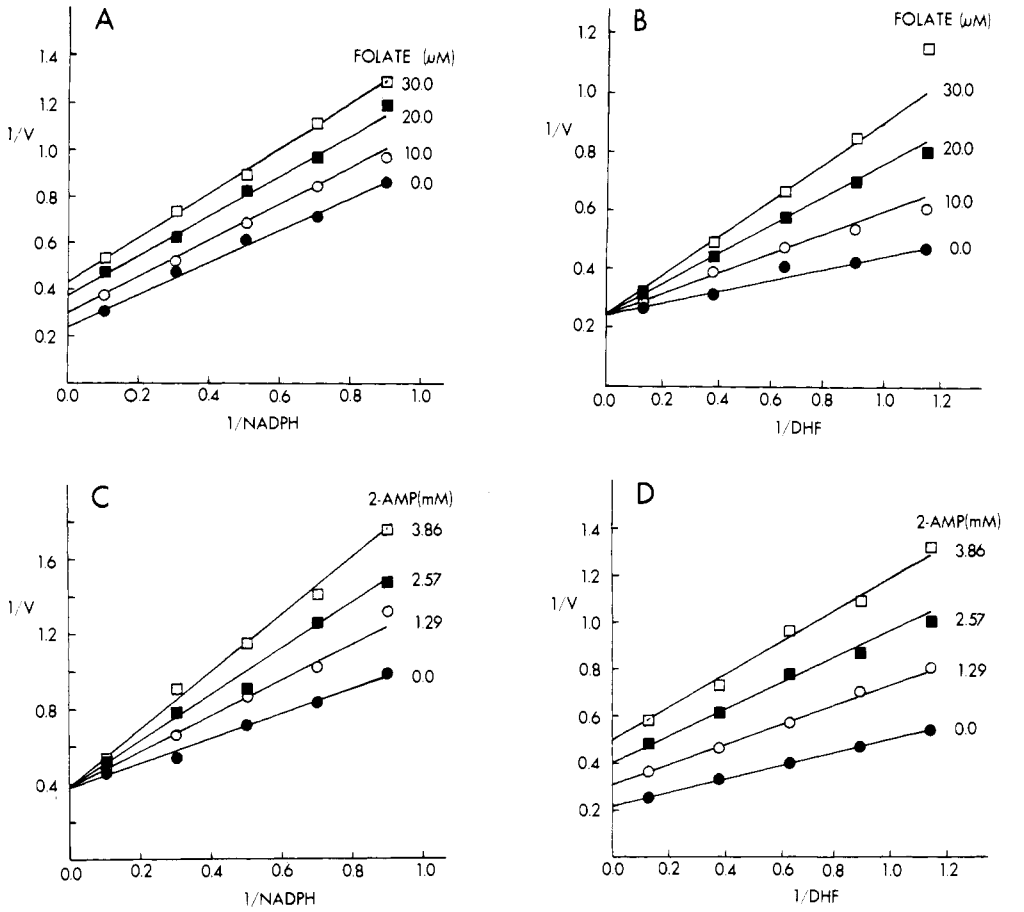

FIGURE 4: Inhibition of the reaction by substrate analogues. Plots of the reciprocal of the initial velocity of the reaction (min × 10^2) against the reciprocal of the concentration of NADPH or DHF ($M^{-1} \times 10^{-6}$). The fixed concentrations of DHF and NADPH were 1.14 μM (A, C) and 3.33 μM (B, D), respectively. The enzyme concentration was 1.8 nM.

only as dead-end inhibitors, the equation that applies can be expressed in reciprocal form as

$$\frac{1}{v} = \frac{1}{V}\left[1 + \frac{K_a}{A}\left(1 + \frac{P}{K_{Ip}} + \frac{Q}{K_{Iq}}\right) + \frac{K_b}{B} + \frac{K_{ia}K_b}{AB}\left(1 + \frac{P}{K_{ip}} + \frac{Q}{K_{iq}}\right)\right] \quad (4)$$

In eq 4, A, B, P, and Q denote concentrations of NADPH, DHF, THF, and NADP, respectively, and K_a and K_b represent Michaelis constants for NADPH and DHF, respectively, while K_{ia} denotes the dissociation constant for the interaction of NADPH with the free enzyme. K_{ip} and K_{iq} represent dissociation constants for the interaction of free enzyme with THF and NADP, respectively, while K_{Ip} and K_{Iq} represent dissociation constants for reaction of the enzyme–DHF complex with THF and NADP, respectively. When relationships derived from eq 4 (cf. Smith & Morrison, 1969) were used, true values were calculated for the kinetic parameters associated with product inhibition (Table III). There is variation in the values of the kinetic constants associated with the reaction of THF with free enzyme (K_{ip}) and with the enzyme–DHF complex (K_{Ip}) as determined in different experiments. However, with both product inhibitors, there is internal consistency with the values for the various kinetic parameters. Thus the calculated values for the complex, competitive inhibition constants (K_{is}) involving either K_{ip} and K_{Ip} or K_{iq} and K_{Iq} are in reasonable agreement with the experimentally determined values. The variation in the values for a particular kinetic constant, as obtained from different types of experiment, may reflect the difficulty of determining precisely values that are in the micromolar region. Alternatively, the variation could be a consequence of the reaction mechanism not being truly rapid equilibrium random (see below).

The dead-end inhibition of dihydrofolate reductase by the substrate analogues, 2′-AMP and folate, can be described by equations of similar form to that of eq 4. Relationships derived from such an equation were used in connection with the determination of true dissociation constants for the interaction of these compounds with both the free and binary forms of enzyme (Table IV). The values indicate that the binding of folate to the free enzyme is strong, although not as strong as DHF (Table II), and that the strength of interaction is enhanced when NADPH is bound to the enzyme. The failure of folate to function as a substrate must be due to lack of hydride transfer from NADPH to folate rather than to lack of folate binding. The binding of 2′-AMP to the enzyme is virtually independent of the DHF concentration and 2–3 orders of magnitude weaker than that of either NADPH or NADP. Thus other moieties of the NADPH molecule make significant contributions to binding. Again, there is reasonable agreement between the calculated and experimentally determined values for K_{is} (Table IV).

Although the results of the analysis of steady-state and progress-curve data are generally consistent with dihydrofolate reductase reaction having a rapid-equilibrium random mechanism, such a description cannot be precise. If catalysis were rate limiting as required for such a mechanism, a ^DV value of 6–10 would be expected. Since a much smaller value of 1.2 was observed, it is apparent that at pH 7.4, product release is not fast relative to the rate of catalysis. The finding that

Scheme II

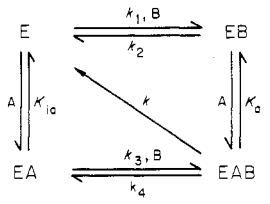

the values for ${}^DV/K_{DHF}$ and ${}^DV/K_{NADPH}$ are lower than that of ${}^DV$ suggests that both substrates may be sticky, so that they react to give products at a rate which is equal to or greater than their rates of dissociation. But some caution must be exercised with respect to this inference because of the small differences between the values. In this connection it is important to note that virtually the same value for the dissociation constant of the enzyme–DHF complex is obtained by kinetic and thermodynamic procedures. However, for the enzyme–NADPH complex, the kinetically determined dissociation constant is about 7-fold greater than the thermodynamic value (Tables II and V). Such findings are in accord with the proposal that the binding of NADPH (A) to the free enzyme and to the enzyme–DHF complex occurs under rapid-equilibrium conditions while the addition of DHF (B) to the free enzyme and to the enzyme–NADPH complex takes place under steady-state conditions (Scheme II). The rate equation for such a mechanism can be derived by using the procedure of Cha (1968) and is expressed as

$$v = \left[\left(\frac{kAE_t}{K_a}\right)\left(k_1B + \frac{k_3AB}{K_{ia}}\right)\right] \Big/ \left[\left[\frac{(k_4 + k)A}{K_a} + k_2\right]\left(1 + \frac{A}{K_{ia}}\right) + \left(k_1A + \frac{k_3AB}{K_{ia}}\right)\left(1 + \frac{A}{K_a}\right)\right] \quad (5)$$

Equation 5 predicts that a primary plot of v^{-1} against B^{-1} will be linear and that a secondary plot of the vertical intercepts against A^{-1} will also be linear and yield a value for K_a. On the other hand, replots of the slopes of the primary plot will be a 2/1 function (Cleland, 1970) in relation to A^{-1} with the horizontal intercept of the asymptote (apparent K_{ia}) being equal to $K_{ia}/[1 + k_3/k_1[K_{ia}K_b/K_aK_{ib} - 1]]$. Thus the kinetically determined values for K_{ia} may be less or greater than the true K_{ia}. If rapid-equilibrium conditions apply, then $K_{ia}K_b = K_aK_{ib}$, and the correct value is obtained for K_{ia} from a slope replot. A primary plot of v^{-1} against A^{-1} will be a 2/1 function, but a secondary plot of the asymptotes will be linear and yield a value for K_{ib} which is equal to k_2/k_1. Thus, for the mechanism described by Scheme II, the kinetic data allow determination of the correct dissociation constant value for the reactant that combines with the free enzyme under steady-state conditions (DHF), but not for that which interacts under rapid-equilibrium conditions (NADPH). Practical problems of data analysis could arise because of difficulties in obtaining data that define the asymptotes of 2/1 plots. But it seems more usual that curvature is not observed in double-reciprocal plots for random mechanisms which do not conform to rapid-equilibrium kinetics. No well-defined curvature was noted in the present study, and yet the aforementioned results, as well as the isotope effects, indicate clearly that the dihydrofolate reductase reaction has a random mechanism which is not of the rapid equilibrium type.

The attention of the authors has been drawn to a recent publication by Cha et al. (1981) in which it was proposed that the reaction catalyzed by dihydrofolate reductase from *Lactobacillus casei* conforms to a rapid-equilibrium random mechanism.

Appendix

Data analysis of progress-curve experiments, consisting of several progress curves, presents some special problems in relation to the estimation of the number of degrees of freedom. Reliable estimates of the kinetic parameters for any one curve will be obtained only if that curve is adequately defined and the obvious way to do this is to take a large number of data points from the curve. However, under these circumstances the standard errors of the parameters will be underestimated because of the overestimation of the degrees of freedom. The latter is theoretically equal to the number of points minus the number of parameters to be determined, provided that the data points are normally and independently distributed. This is not the case with progress-curve data. An accurate representation of the degrees of freedom is also necessary for application of the variance ratio (F) test in choosing between models.

Duggleby & Morrison (1978) circumvented the aforementioned problem by fitting data from a single progress curve to eq 1 and using the resulting parameter values to compress the data into three points. The same procedure has been used in the present study, but further consideration has been given to the location of the three points. For the three points to represent adequately a progress curve described by eq 1, they must be chosen so that each of the three terms of the equation is dominant in one of the points. In general, this will occur for R_1 at the beginning, and for R_2 and R_3 toward the end, of the progress curve. However, there will be an influence of the magnitude of the R values.

Condition 1 of the present study follows the suggestion of Duggleby & Morrison (1978) that points be taken from the progress curve at the beginning, after 95% utilization of substrate and at a time halfway between the two extremes. When this procedure was used, the mechanisms yielding the lowest residual sums of squares were rapid-equilibrium random and rapid-equilibrium ordered mechanisms with each involving a dead-end enzyme–DHF–THF complex. The two mechanisms differed in that the equation describing the rapid-equilibrium random mechanism contained an additional K_b ln $(1 - P/B)$ term. The results of an F test showed that the reduction in the residual sums of squares by inclusion of the additional term was not significant, and thus the rapid-equilibrium ordered mechanism was to be preferred. However, care must be exercised when choosing between models on the basis of an F test for the data can be ill-conditioned with respect to the determination of the parameter whose significance is being tested. So that this point could be tested with respect to K_b, data from individual progress curves were compressed so that one of the points was taken at 98% (condition 2), rather than 95% (condition 1), utilization of substrate. Under this condition the value of ln $(1 - P/B)$ will increase and the data will be better conditioned for the determination of K_b if that parameter is significant. Analysis indicated that this was the case.

The difference in the results obtained under the two conditions of data compression emphasizes the fact that a single set of conditions cannot be used for all progress-curve experiments. It is proposed that initial estimates of the parameters be obtained under one condition of data compression and that, in the light of these results, the conditions of data compression be varied so as to optimize the determination of each parameter. This procedure is equivalent to the variation of substrate concentration in steady-state kinetics so as to allow accurate determination of parameter values.

The present study has demonstrated that the analysis of progress-curve data can be a useful procedure for studying enzymes with Michaelis constants that are micromolar or lower. Although the results did not permit an unequivocal choice of mechanism, nevertheless, they did allow elimination of several mechanisms from further consideration. The results also provided good estimates of parameter values which were of use in connection with the definitive elucidation of the mechanism of the dihydrofolate reductase reaction by steady-state techniques.

References

Birdsall, B., Griffith, D. V., Roberts, G. C. K., Feeney, J., & Burgen, A. (1977) *Proc. R. Soc. London, Ser. B 196*, 251–265.

Blakley, R. L. (1960) *Nature (London) 188*, 231.

Blakley, R. L. (1969) *The Biochemistry of Folic Acid and Related Pteridines*, North-Holland Publishing Co., Amsterdam.

Blakley, R. L., Schrock, M., Sommer, K., & Nixon, P. F. (1971) *Ann. N.Y. Acad. Sci. 186*, 119–130.

Burchall, J. J., & Chan, M. (1969) *Fed. Proc., Fed. Am. Soc. Exp. Biol. 28*, 352.

Cha, S. (1968) *J. Biol. Chem. 243*, 820–825.

Cha, S., Kim, S. Y. R., Kornstein, S. G., Kantoff, P. W., Kim, K. H., & Naguib, F. N. M. (1981) *Biochem. Pharmacol. 30*, 1507–1515.

Cleland, W. W. (1970) *Enzymes, 3rd Ed. 2*, 1–65.

Dawson, R. M. C., Elliott, D. C., Elliott, W. H., & Jones, K. M. (1969) *Data for Biochemical Research*, Oxford University Press, Oxford.

Duggleby, R. G., & Morrison, J. F. (1977) *Biochim. Biophys. Acta 481*, 297–312.

Duggleby, R. G., & Morrison, J. F. (1978) *Biochim. Biophys. Acta 526*, 398–409.

Duggleby, R. G., & Morrison, J. F. (1979) *Biochim. Biophys. Acta 568*, 357–362.

Gready, J. E. (1980) *Adv. Pharmacol. Chemother. 17*, 37–102.

Hillcoat, B. L., Nixon, P. F., & Blakley, R. L. (1967) *Anal. Biochem. 21*, 178–189.

Matthews, D. A., Alden, R. A., Bolin, J. T., Filman, D. J., Freer, S. T., Hamlin, R., Hol, W. G. J., Kisliuk, R. L., Pastore, E. J., Plante, L. T., Xuong, N.-H., & Kraut, J. (1978) *J. Biol. Chem. 253*, 6946–6954.

McCullough, J. L., Nixon, P. F., & Bertino, J. R. (1971) *Ann. N.Y. Acad. Sci. 196*, 131–142.

Pollard, J. H. (1977) *Numerical & Statistical Techniques*, pp 309–311, Cambridge University Press, Cambridge.

Rood, J. I., & Williams, J. W. (1981) *Biochim. Biophys. Acta 660*, 214–218.

Rood, J. I., Laird, A. J., & Williams, J. W. (1980) *Gene 8*, 255–265.

Selwyn, M. J. (1965) *Biochim. Biophys. Acta 105*, 193–195.

Smith, E., & Morrison, J. F. (1969) *J. Biol. Chem. 244*, 4224–4234.

Smith, E., & Morrison, J. F. (1971) *J. Biol. Chem. 246*, 7764–7772.

Viola, R. E., Cook, P. F., & Cleland, W. W. (1979) *Anal. Biochem. 96*, 334–340.

Williams, J. W., Morrison, J. F., & Duggleby, R. G. (1979) *Biochemistry 18*, 2567–2573.

Williams, J. W., Duggleby, R. G., Cutler, R., & Morrison, J. F. (1980) *Biochem. Pharmacol. 29*, 589–595.

Zakrzewski, S. F., & Sansone, A. M. (1971) *Methods Enzymol. 18B*, 728–731.

3-Fluoro-3-deoxycitrate: A Probe for Mechanistic Study of Citrate-Utilizing Enzymes†

Steven E. Rokita, Paul A. Srere, and Christopher T. Walsh*

ABSTRACT: The interaction of a novel fluorinated analogue of citrate, 3-fluoro-3-deoxycitrate (3-fluorocitrate), with the four known citrate-processing enzymes is described in this report. Three of the citrate-processing enzymes, citrate synthase, ATP citrate lyase, and citrate lyase, catalyze reversible aldol-type condensations. The fate of 3-fluorocitrate with each enzyme is uniquely related to their mechanisms of action. For citrate synthase, 3-fluorocitrate is a competitive inhibitor. 3-Fluorocitrate is a substrate for the carboxylate activation half-reaction catalyzed by ATP citrate lyase and induces a net ATPase action during conversion to 3-fluorocitryl-S-coenzyme A. Because of the unusual mechanism of citrate cleavage catalyzed by bacterial citrate lyase, 3-fluorocitrate is a mechanism-based inhibitor, acting at two points during turnover of the acetyl enzyme. The fourth citrate-processing enzyme, aconitase, does turn over 3-fluorocitrate catalytically. This enzyme, catalyzing a dehydration and rehydration of citrate, also catalyzes the elimination of HF from 3-fluorocitrate, yielding *cis*-aconitate and fluoride.

Citrate, **1**, is a central component in the primary metabolism of prokaryotes and eukaryotes. It is processed by only four enzymes and undergoes two types of transformations (Goodwin, 1968). Three enzymes carry out reversible aldol-type cleavage of the 3-hydroxytricarboxylate skeleton to yield the C_2 (acetate or acetyl-CoA)[1] and the C_4 (oxalacetate) fragments. These are bacterial citrate lyase (EC 4.1.3.6), mam-

† From the Departments of Chemistry and Biology, Massachusetts Institute of Technology, Cambridge, Massachusetts 02139 (S.E.R. and C.T.W.), and the Department of Biochemistry and Veterans Administration Medical Center, The University of Texas Health Science Center at Dallas, Dallas, Texas 75235 (P.A.S.). *Received December 28, 1981.* This investigation was supported in part by National Institutes of Health Grant GM 20011.

[1] Abbreviations: HPLC, high-performance liquid chromatography; CoA, CoASH, or $CoAS^-$, coenzyme A; NADH, reduced nicotinamide adenine dinucleotide; $NADP^+$, nicotinamide adenine dinucleotide phosphate; cpm, counts per minute; 3-fluorocitrate, 3-fluoro-3-deoxycitrate; unit, enzyme unit defined to be the quantity of enzyme necessary to transform 1 μmol of substrate in 1 min; Tris, tris(hydroxymethyl)-aminomethane.

0006-2960/82/0421-3765$01.25/0